

A NOVEL METHOD FOR ROBUST ESTIMATION OF GROUP FUNCTIONAL CONNECTIVITY BASED ON A JOINT GRAPHICAL MODELS APPROACH

Xiaoyun Liang¹, Alan Connolly^{1,2}, and Fernando Calamante^{1,2}

¹Brain Research Institute, Florey Institute of Neuroscience and Mental Health, Melbourne, VIC, Australia, ²Department of Medicine, Austin Health and Northern Health, University of Melbourne, Melbourne, VIC, Australia

Introduction: Increasing evidence suggests that human brain can be modeled as a complex network [1]. Advances in graph theory have provided a powerful tool to characterize (functional and structural) brain networks and connectivity. In this context, functional connectivity has been estimated mainly through calculating cross-correlation coefficients of fMRI signal between pairs of parcellated brain regions [2]. However, this approach measures the general relationship between two regions without taking account of the influence of the others. While this issue could be addressed, in principle, by using partial correlations, it is not suitable for cases with large number of regions; this is exacerbated when the number of possible connections is larger than the available number of time points, which is usually the case for functional connectivity studies. Since estimating partial correlations is equivalent to estimating the inverse covariance matrix, regularization strategies that provide sparse solutions have been proposed for estimating the inverse covariance matrix, and thus connections [3]. Furthermore, to obtain networks at group level, networks calculated at individual level are usually averaged across the group. This is inevitably affected by inter-subject variability, which is made worse by the relatively low SNR of fMRI data. To address these issues, we propose to use a joint sparsity constraint method with joint graphical models (JGM) [4] to directly estimate a *group-level* inverse covariance matrix, therefore accounting for inter-subject variability. To circumvent the issue of choosing regularization parameters, a recently proposed stability selection method is employed [5]. The proposed method, combining JGM with stability selection (labeled JGMSS) is first assessed using simulated data and then applied to *in vivo* fMRI data. For comparison, a recent regularization method using elastic net (EN) penalty [3] was also applied to both simulated and *in vivo* data.

Methods: The JGM can be described as follows [4]. Assuming that K datasets, $X^{(1)}, \dots, X^{(K)}$, are obtained, $X^{(k)}$ is an $n_k \times p$ matrix, with n_k representing time points of fMRI data, and p the number of brain regions. The empirical covariance matrix for $X^{(k)}$ can then be calculated as: $S^{(k)} = 1/n_k (X^{(k)})^T X^{(k)}$. Maximum likelihood estimate of $(S^{(k)})^{-1}$ can be obtained by estimating $\{\Theta\}$ with the following equation: $\max_{\{\Theta\}} (\sum_k n_k \log(\det(\Theta^{(k)}) - \text{tr}(S^{(k)}\Theta^{(k)})) - P(\{\Theta\})$, $k=1, \dots, K$, with the constraint that all $\hat{\Theta}^{(k)}$ are positive definite. Here, group graphical lasso, $P(\{\Theta\}) = \lambda_1 \sum_k \sum_{i \neq j} |\theta_{ij}^{(k)}| + \lambda_2 \sum_k (\sum_{i \neq j} |\theta_{ij}^{(k)}|)^{1/2}$, where λ_1 and λ_2 are non-negative regularization parameters, and $k=1, \dots, K$. By applying the penalty, it encourages a similar pattern of sparsity across the K precision matrices. To estimate the group-level precision matrix, an alternating direction method of multipliers was employed [4, 6]. Given that it is difficult to determine optimal regularization parameters, λ_1 and λ_2 , a stability selection method is employed to estimate stable connections [5]. With stability selection, the data are subsampled many times and all variables that occur in a large fraction of the resulting selection sets are selected. For regularization parameters (λ_1, λ_2) , the estimated connectivity matrix is denoted as $S^{\lambda_1, \lambda_2} = \{(m, n) : 1 \leq (m, n) \leq M; \Theta(m, n) \neq 0\}$. For a cut-off $\pi_{thr} \in (0, 1)$ and a set of regularization parameters, the set of stable connections are as follows: $\hat{S}^{\text{stable}} = \{(m, n) : \max_{\lambda_1, \lambda_2} \hat{\pi}_{m, n}^{\lambda_1, \lambda_2} \geq \pi_{thr}\}$.

To demonstrate the robustness of the proposed method, simulations were conducted according to ref [7]. **Simulation:** Networks of small-world properties were simulated with 5 different percentages of connections ($r=16, 24, 28$ and 32). The number of regions and observations are $p=50$ and $n=56$, respectively. For each r , the procedure was repeated 10 times to generate 10 datasets. To perform stability selection, $n/2$ observations were randomly subsampled without overlapping for each dataset, which was repeated 100 times to estimate the probabilities $\hat{\pi}_{m, n}^{\lambda_1, \lambda_2}$ over the regularization region $\Lambda(\lambda_1, \lambda_2)$. It has been shown that the expected number of falsely selected connections V is bounded by $E(V) = 1/(2\pi_{thr} - 1)q^2/p$ [5], where p is the total number of variables in the model and q is the average number of selected connections for a given range of (λ_1, λ_2) . The per-comparison error rate ($PCER = E(V)/p$) is employed to control falsely selected connections. **In vivo data:** Arterial spin labeling (ASL) fMRI data were acquired in ten subjects on a 3T Siemens Trio scanner using a whole-brain 3D-GRASE pCASL sequence [8]; TR/TE=3750/56ms, resolution = $4 \times 4 \times 6 \text{ mm}^3$, 20 slices, matrix size = 64×51 , post-labeling delay=600ms, with labeling duration = 1284ms. Background suppression was achieved using TIs= 1913ms and 523ms [8]. In addition, anatomical and calibration images were acquired for registration and CBF quantification. **Image analysis:** ASL perfusion images were pre-processed as follows [8]: realignment, coregistration, normalization (MNI template, $61 \times 73 \times 61$), independent component analysis was performed using MELODIC in FSL. The pre-processed ASL perfusion images were employed as inputs to calculate node-wise mean time series at individual level where AAL template (84 ROIs [9]) was used to define the nodes. With these individual-level time series as inputs, the proposed method was then employed for estimating group-level functional networks. Since fMRI signal is not independent, the time series were divided into 14 consecutive blocks (4 time points each block). For comparisons, regularization using EN penalty [3] was also applied. The $PCER (=0.05$ for $PC=16\%$, 0.1 otherwise due to inaccessible $\pi_{thr} > 1$) was employed to control falsely selected connections. To investigate the legitimacy of choosing π_{thr} by setting $PCER$, an optimal estimate of network (with a maximum accuracy rate) was calculated based on ground truth for each simulation. For *in vivo* data, $PCER=0.05$ was used to determine π_{thr} for controlling falsely selected connections.

Results: Fig. 1 shows that JGMSS can estimate networks with consistently higher accuracy and sensitivity than EN within the varying range of r . Moreover, JGMSS achieves near optimal accuracy and sensitivity (as determined based on ground truth) by controlling falsely selected connections; EN, however, deviates far from its optimal estimates (Fig. 1). Fig. 2 illustrates examples of network estimation using JGMSS (left) and EN (middle), with a true (simulated ground truth) network (right). It clearly demonstrates that JGMSS can more reliably estimate true connections than EN does. While JGMSS generally introduces slightly higher false positive rate, the consistently higher accuracy and sensitivity confirms the validity of JGMSS for estimating networks at group-level. For *in vivo* data, networks were estimated for JGMSS (Fig. 3, top middle) and EN (Fig. 3, bottom middle) by setting $PCER=0.05$. Networks estimated with 2 other π_{thr} (0.7 and 0.9) are also shown (Fig. 3). While the estimated networks using EN are largely dependent on π_{thr} , those estimated using JGMSS varies little with π_{thr} (Fig. 3). Calculation of small-world index ($\pi_{thr} = 0.7-0.95$, 0.05 each step) further confirms much less dependence of JGMSS on the π_{thr} than EN (Fig. 4).

Discussion: In this study, we proposed a joint sparsity constraint method using JGMSS to directly estimate networks at group-level. Simulations demonstrate that JGMSS can achieve consistently higher accuracy and sensitivity than EN. Notably, simulated results show fairly low accuracy and sensitivity with EN compared to another study [3]. This is likely due to much fewer time points (56 vs 200) and number of subjects (10 vs 50) in our study. This further demonstrates the power of JGMSS in reliable network estimation, even in such cases. Since choosing appropriate threshold is still an open question, $PCER$ was employed to choose a threshold for stability selection. Near optimal estimates of networks using JGMSS have been confirmed with simulations. Furthermore, our results show much less network variability (Fig. 3 and 4) across the selected range of threshold (0.7-0.95) than EN does, suggesting that JGMSS is relatively insensitive to threshold. Furthermore, based on simulated results (Fig. 2), JGMSS was found to achieve higher sensitivity, although it tends to estimate more false connections than EN. Therefore, it is more likely that choosing π_{thr} by controlling $PCER$ is a near optimal way for JGMSS than for EN for *in vivo* data. Overall, JGMSS can robustly and reliably estimate functional connectivity at group-level. Finally, it should be noted that, while JGMSS was illustrated here with ASL fMRI data, the proposed method can be directly applied to BOLD-based studies.

References: [1] Stam CJ et al., *NeuroImage* 2006; 32: 1335-44; [2] Achard S et al., *J. Neuroscience* 2006; 26: 63-72; [3] Ryali S et al., *NeuroImage* 2012; 59: 3852-61; [4] Danaher P et al., *J. R. Statist. Soc. B* 2013; [5] Meinshausen N et al., *J. R. Statist. Soc. B* 2010; 72(4): 417-73; [6] Boyd S, *Foundations and Trends in Machine Learning* 2010; 3(1): 1-122; [7] Peng J et al. *J. Am. Statist. Assoc.* 2009; 104(486): 735-46; [8] Liang X et al., *Int. J. Imag. Syst. Tech.* 2012; 22(1): 37-43; [9] Liang X et al., *NeuroImage* (in press).

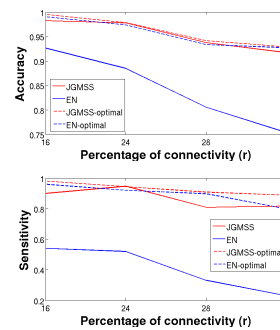


Figure 1

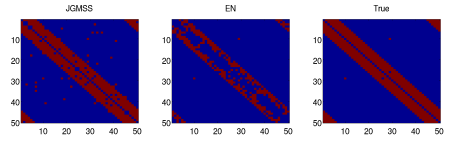


Figure 2

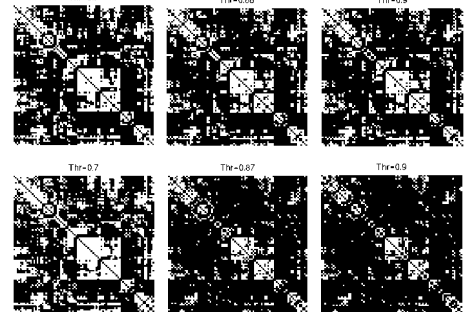


Figure 3

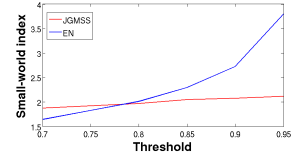


Figure 4